Colloids and Surfaces B: Biointerfaces 81 (2010) 235–241

Contents lists available at ScienceDirect

Colloids and Surfaces B: Biointerfaces

journal homepage: www.elsevier.com/locate/colsurfb

Functionalization of gold nanoparticles with amino acid, β-amyloid peptides and fragment

A. Majzik[a], L. Fülöp[b], E. Csapó[a], F. Bogár[b], T. Martinek[c], B. Penke[a,b], G. Bíró[d], I. Dékány[a,d,*]

[a] Supramolecular and Nanostructured Materials Research Group of the Hungarian Academy of Sciences, University of Szeged, 6720 Szeged Aradi vt. 1, Hungary
[b] Department of Medical Chemistry, University of Szeged, H-6720 Szeged, Dóm t. 8, Hungary
[c] Institute of Pharmaceutical Chemistry, University of Szeged, H-6720 Szeged, Eötvös u. 6, Hungary
[d] Department of Physical Chemistry and Materials Sciences, University of Szeged, H-6720 Szeged, Aradi vt. 1, Hungary

ARTICLE INFO

Article history:
Received 10 January 2010
Received in revised form 18 May 2010
Accepted 7 July 2010
Available online 13 July 2010

Keywords:
Au nanoparticles
Cysteine
β-Amyloid peptides
Aggregation

ABSTRACT

Gold nanoparticles (Au NPs) were functionalized by cysteine (*Cys*), β-amyloid peptides (*$Cys^0A\beta_{1-28}$*, *$Cys^0A\beta_{1-40}$*, *$A\beta_{1-42}$*) and a pentapeptide fragment (*Leu-Pro-Phe-Phe-Asp-OH* (*LPFFD-OH*)). Optical absorption spectra of these systems were recorded and the plasmon resonance maximum values (λ_{max}) of the UV–vis spectra together with the transmission electron microscopy (TEM) images were also analysed. Both TEM images and the appearance of a new absorption band between ~720 and 750 nm in the visible spectra of the Au–cysteine and Au–LPFFD-OH systems most probably indicate that upon addition of these molecules to Au NPs-containing aqueous dispersions formation of aggregates is occurred. The wavelength shift between the two observed absorption bands in cysteine- and pentapeptide-modified Au NPs systems are $\Delta\lambda = 185$ and 193 nm, respectively. These results suggest that the monodisperse spherical gold nanoparticles were arranged to chained structure due to the effect of these molecules. For confirmation of the binding of citrate and cysteine onto the plasmonic metal surface ^{1}H NMR measurements were also performed. ^{1}H NMR results may suggest that the citrate layer on the metal surface is replaced by cysteine leading to a formation of organic double layer structure.

In the presence of β-amyloid peptides the aggregation was not observed, especially in the Au–$Cys^0A\beta_{1-40}$ and Au–$A\beta_{1-42}$ systems, however compared to the cysteine or LPFFD-OH-containing gold dispersion with $Cys^0A\beta_{1-28}$ measurable less aggregation were occurred. The spectral parameters clearly suggest that $A\beta_{1-42}$ can attach or bind to the surface of gold nanoparticles via both the apolar and the N-donors containing side-chains of amino acids and no aggregation in the colloidal gold dispersion was observed.

1. Introduction

Numerous methods for preparation of noble (Au, Ag) nanoparticles (NPs) are found in the literature [1,2]. It is also well-known that the spectral parameters of NP-containing dispersions also depend on the size and shape of the particles [3,4]. For example, in the case of Au NPs (particle diameter ~10–20 nm) the observed absorbance maximum (λ_{max}) in the visible spectrum is ~525 nm [1,2]. Parallel with enlargement of the size and/or formation of aggregates, a red shift of the band or appearance of other new plasmon band at higher wavelength can be also observed [1,3].

The interaction of gold and silver nanoparticles with biomolecules has been intensively studied for many years [5,6]. Since metal nanoparticles emit surface plasmon oscillations in the visible wavelength range, their optical properties attract intense scientific and technological interest [7]. In most cases citrate-based gold nanoparticles were used in numerous biological studies. These nanoparticles are stabilized by a citrate ligand layer through electrostatic interactions. Due to the only electrostatic effects of citrate adsorption binding of proteins and other biomolecules on the NPs surface is possible [8].

Among other research groups, Zhong et al. [9] showed that gold nanoparticles reduced and stabilized by citrate have a negatively charged surface and preferentially bind to molecules including thiol, amine, cyanide or diphenylphosphine functional groups. They also observed that the reactivity of the amino group of amino acids was pH-dependent. Binding of α-amino groups is preferential at especially low pH, while the role of this group is negligible at neutral and high pH. Further investigations of this research group also

* Corresponding author at: Supramolecular and Nanostructured Materials Research Group of the Hungarian Academy of Sciences, University of Szeged, 6720 Szeged Aradi vt. 1, Hungary.
E-mail address: i.dekany@chem.u-szeged.hu (I. Dékány).

0927-7765/$ – see front matter © 2010 Elsevier B.V. All rights reserved.
doi:10.1016/j.colsurfb.2010.07.011

showed that dibasic amino acids can be used to cross-link Au colloids at high pH [9].

Aryal et al. [10] prepared approximately ~12 nm gold nanoparticles by borohydride reduction. For the spectroscopic identification of S–Au binding in aqueous medium, UV–vis, Raman, NMR and FT-IR spectroscopy techniques were performed. These spectroscopic results clearly showed that the thiol moiety of cysteine is a very effective site to interact with gold. Due to this interaction cysteine-capped gold nanoparticles are formed [10]. In addition, the electrolyte induced aggregation of different amino acid-capped gold nanoparticles (L-cysteine, L-leucine, L-asparagine) was also investigated. Due to the increase of electrolyte concentration and decrease of pH, both the red shift and the broadening of surface plasmon band parallel with the increase in the flocculation parameter suggested that an aggregation of gold nanoparticles occurred. The ^{1}H NMR spectra demonstrated that the sulfhydrile group of cysteine and amino moiety of leucine and asparagine also represent a measurable interaction with Au nanoparticles [11].

Porta et al. [12] applied two dipeptides (Gly-Lys and Gly-Cys) and two 15 amino acid-long peptides (GK15 and GC15) as capping agents for preparation of monolayer-protected gold nanoparticles. The capped-NPs were characterized by TEM images, UV–vis, NMR and IR spectroscopy. Formation of Au–citrate-GC15 bioconjugates (red sol) was observed during the reaction of citrate-capped gold dispersion with GC15. However, NMR and IR studies confirmed the presence of capping agents in bioconjugate but did not indicate a well-defined interaction of GC15 with gold [12].

Gold surfaces are also suitable for studying peptide-peptide or peptide-protein interactions using surface plasmon resonance (SPR) spectroscopy. It is also well-known that Alzheimer's β-amyloid (1-42) peptide ($A\beta_{1\text{-}42}$) is capable for interaction with numerous intracellular and extracellular molecules; however, the relative contribution of these interactions to the toxicity of Aβ is not clearly understood. In order to characterize the complicated mechanisms and also the effects of interactions between $A\beta_{1\text{-}42}$ and the above mentioned molecules, numerous groups have focused their research on these investigations.

Several Aβ peptides can be immobilized on gold surfaces [13–17]. The kinetics of amyloid aggregation (from monomers to fibrils) and also the effect(s) of metal ions in the case of aggregation process were also extensively investigated [18–21]. Interactions between gold surfaces-immobilized Aβ-peptides and gangliosides [22], flavonoids [23], tau-protein [17] and alcohol dehydrogenase [24] were also studied in previous literatures. Aβ-peptides coupling onto gold surface are potent bioconjugates to study the binding of different drug candidates on Aβ species [13,25]. In an excellent review, the application of SPR for the analysis of Aβ interactions and fibril formation in Alzheimer's disease research was summarized [26]. In this report, interaction of $A\beta_{1\text{-}42}$ with small biomolecules and proteins was investigated. Despite of the efforts, a detailed mechanism of interaction of $A\beta_{1\text{-}42}$ with gold nanoparticles is not fully resolved, yet. For determining the binding affinity of novel drug candidates onto toxic $A\beta_{1\text{-}42}$ aggregates, a well characterized aggregation state of $A\beta_{1\text{-}42}$ immobilized on gold nanoparticles is extremely important as well.

In the work presented here, size-controlled gold nanoparticles (reduced and stabilized by citrate) were prepared in aqueous dispersions. The interaction of the cysteine (Cys), LPFFD-OH pentapeptide (peptide inhibitor iAβ5-OH [27]), cysteine modified β-amyloid (1-28) ($Cys^0A\beta_{1\text{-}28}$), β-amyloid (1-40) ($Cys^0A\beta_{1\text{-}40}$) and $A\beta_{1\text{-}42}$ on gold nanoparticles were studied. In order to determine the effects of these biomolecules with Au NPs the shift of plasmon resonance maximum values detected in the UV–vis spectra together with the TEM images were analyzed. NMR spectroscopy was used to study the interactions between small molecules and citrate-stabilized gold NPs-containing dispersion.

2. Materials and methods

LPFFD-OH, $Cys^0A\beta_{1\text{-}28}$, $Cys^0A\beta_{1\text{-}40}$, $A\beta_{1\text{-}42}$ biomolecules were prepared in our laboratory by applying methods reported previously [28]. L-Cysteine (≥99.5%) was purchased from Fluka and used without any further purification.

2.1. Preparation of gold nanoparticles

0.24 cm^3, 0.05 M $HAuCl_4 \times 3H_2O$ (Sigma–Aldrich) was diluted with 58 cm^3 MilliQ water and brought to boil, while kept under vigorous stirring. Sodium citrate (Reanal, Hungary) (1.71 cm^3, 0.035 M) was added to this solution and the dispersion was stirred for 30 min (Au:citrate molar ratio was 1:5). During the reduction, the colour of the sample was changed from faint yellowish to wine-red. The sodium citrate was applied as reducing agent but this molecule also stabilizes the gold nanodispersion yielding a negatively charged gold surface. Due to this negatively charged double layer, stable Au NPs-containing aqueous dispersion was formed and aggregation did not occur. For observation of the gold nanoparticles, UV–vis measurement was performed. The absorbance maximum of the plasmon band appearing in the spectrum was at $\lambda_{max} \sim 530$ nm, which result is in good agreement with the earlier findings in the literature [1,2].

2.2. Measurement methods

A diode array spectrophotometer (Ocean Optics Chem 2000-UV–vis) was used for characterization of the effects of Cys, LPFFD-OH, $Cys^0A\beta_{1\text{-}28}$, $Cys^0A\beta_{1\text{-}40}$ and $A\beta_{1\text{-}42}$ with gold nanoparticles at λ = 200–850 nm wavelength range using an 1 cm quartz cuvette.

Particle size distribution was determined by dynamic light scattering (DLS) using a Zetasizer Nano ZS ZEN 4003 apparatus (Malvern Instrument, UK). The measurements were recorded at 25 ± 0.1 °C. Since the zeta-potential studies were performed in aqueous solution, the Smoluchowski approximation was used to calculate the zeta-potentials with the aid of the electrophoretic mobility values.

Transmission electron microscope (TEM) images were recorded on a Philips CM-10 TEM instrument at 100 kV accelerating voltage. The microscope was equipped with a Megaview II digital camera. Samples were analyzed on Formvar-coated copper grids. The size distribution of the particles was calculated by using UTHSCSA Image Tool 2.00 software.

^{1}H NMR measurements for cysteine and Au NPs–cysteine systems have been performed on Bruker Avance 500 instrument at 298 K. The spectra were acquired with the WATERGATE solvent suppression pulse scheme. Noble metal NPs to cysteine ratio was 1:50 and the analytical concentration of Cys was 10 mM in all samples, while the pH was adjusted to 6.0.

3. Results and discussion

It is well-known, that for preparation of Au NPs, parallel with the change of the Au:citrate ratio, the size of the particles is controllable. In this work, an 1:5 Au:citrate molar ratio was used yielding Au NPs with d_{Au} = 13.6 ± 4.7 nm average diameter, as was proven by TEM images. Formation of these nanoparticles was also followed by DLS measurements. The average particle diameter was 18.21 ± 4.3 nm measured by this method. The Zeta-potential of the prepared gold dispersion at pH = 6 was also determined, and the value (ζ = −41.8 ± 2.01 mV) was in good agreement with the earlier findings in the literature [29]. This potential value was also confirmed the formation of negatively charged surface in this citrate-stabilized gold dispersion at pH = 6.

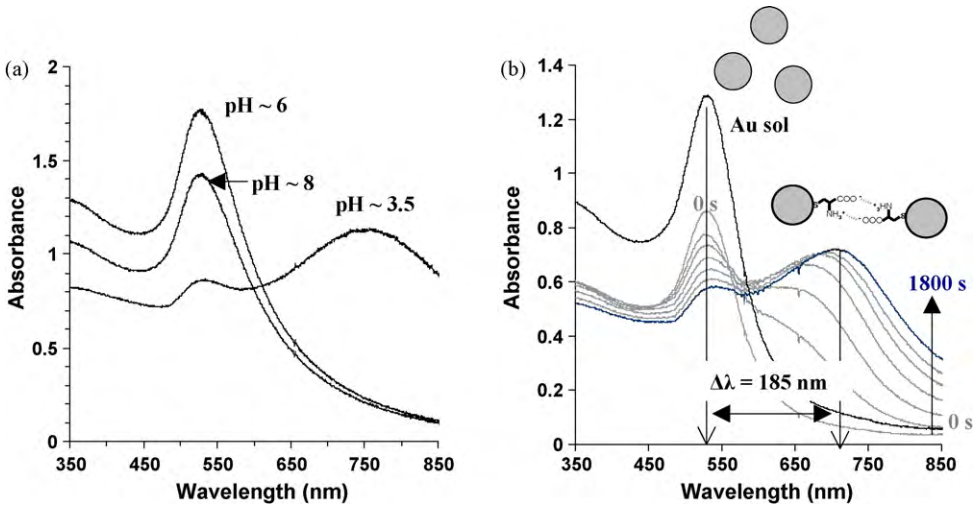

Fig. 1. UV–vis spectra recorded for the Au–cysteine 1:5 system as a function of pH (a) and the spectra of Au–cysteine 1:5 system registered at pH ~ 3.5 at different time (b) (c_{Au} = 0.4 mM, $c_{citrate}$ = 2 mM and c_{Cys} = 2 mM).

3.1. Surface modification of gold nanoparticles by cysteine

Before characterization of the effect of β-amyloid peptides with gold nanoparticles, we started to investigate the effect of smaller biomolecules like cysteine and the LPFFD-OH pentapeptide. In the case of Au–cysteine system, the registered UV–vis spectra at different pH values are presented in Fig. 1a. As it can be seen in Fig. 1a, only one plasmon resonance band with λ_{max} at 529 nm exists above pH ~ 6, but the presence of a new band at ~715 nm is observed at acidic pH. This new band in the spectra suggests the formation of aggregates of gold nanoparticles due to the electrostatic interaction of the negatively charged carboxylate and positively charged amino groups. Above pH ~ 6, parallel with the deprotonation of the ammonium group, the aggregation is not observed.

Fig. 1b presents the spectra recorded for 1:5 Au–Cys ratio at 3.5 in different time points. The spectrum with the largest absorbance maximum corresponds to the original spherical gold NP-containing dispersion. After addition of cysteine to the dispersion the change in the UV–vis spectrum with time was registered. As it is shown in Fig. 1b, two seconds after the administration of Cys, a new plasmon maximum starts to increase, while the peak at ca. 530 nm gradually decreases. Most probably the cysteine molecules are binded to the surface of gold nanoparticles via their thiol groups, while electrostatic interaction between the protonated amino group and deprotonated carboxylic moiety occurs as well. This interaction is demonstrated also in Fig. 1b. The wavelength distance between the two observed band (λ_{max1} = 530 nm, λ_{max2} = 715 nm) is $\Delta\lambda$ = 185 nm, which suggests that the nanoparticles are arranged in chains by the effect of the cysteine molecules and dominance of the chain-like aggregated structure is persistent in this system at pH ~ 3.5. Comparison of TEM images of Fig. 2a and b it can be seen, that by adding cysteine to the stable gold dispersion, formation of the above mentioned aggregates occurs, which is also confirmed by the change in the colour of the sample (from pink to blue).

In order to characterize the binding of the cysteine molecule to gold surface, ^{1}H NMR measurements were performed. The spectra of the citrate-stabilized gold aqueous dispersion (1) and the cysteine molecule (3) can be seen in Fig. 3. This figure also shows the spectrum of the Au–Cys system (2). The registered spectra for this Au–Cys system showed that the intensity of the signals of the citrate–CH_2 (assigned with C) substantially decreased and broadened due to the addition of cysteine while there was no change in the intensity of the cysteine signals. These experimental findings may suggest that most of the citrate molecules on the gold surface are replaced by cysteine yielding the formation of a "double organic layer" structure in the applied concentration. One possible schematic representation of this "double organic layer" structure is presented in Fig. 4.

3.2. Surface modification of gold nanoparticles by β-amyloid peptides and a pentapeptide

Citrate-stabilized surface of gold nanoparticles were also modified with a pentapeptide Leu-Pro-Phe-Phe-Asp (LPFFD-OH). This molecule cannot form covalent bonds with the surface; only elec-

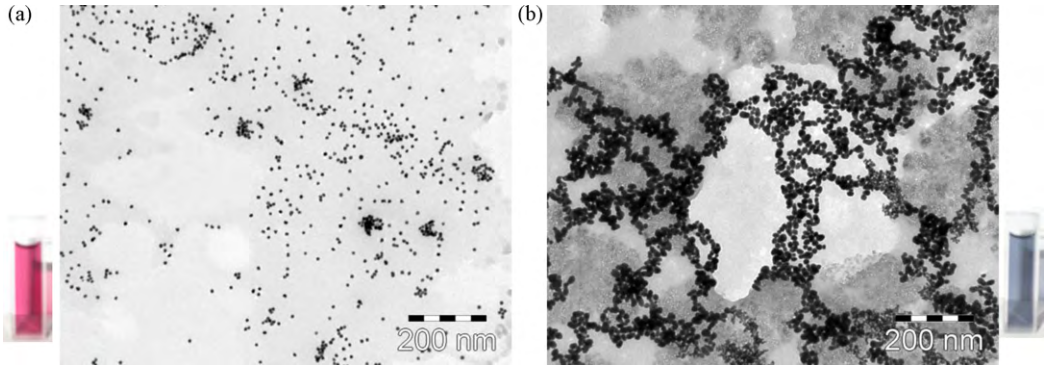

Fig. 2. TEM images of the prepared citrate-stabilized gold nanodispersion before (a) and after (b) addition of cysteine at 46,000× enlargement (a: c_{Au} = 0.4 mM, b: c_{Au} = 0.4 mM, c_{Cys} = 2 mM).

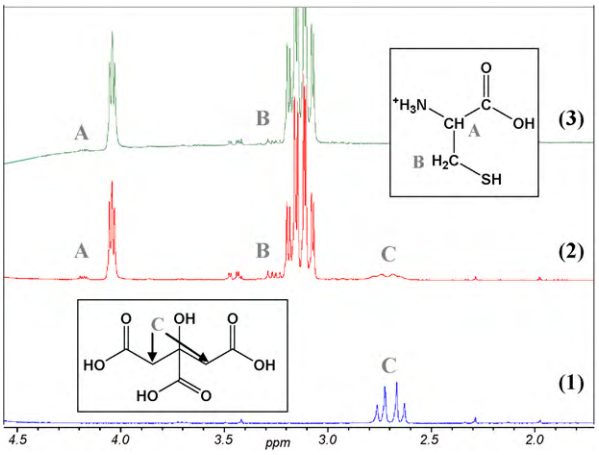

Fig. 3. Representative ^{1}H NMR spectra of citrate-stabilized gold nanodispersion (1), cysteine (3) and Au–cysteine system (2) (c_{Au} = 0.2 mM, $c_{citrate}$ = 2 mM, c_{Cys} = 10 mM) Letter A relates *CH*, B for CH_2 protons of the cysteine, while C relates CH_2 protons of citrate.

trostatic interaction is possible with the gold particles, because the surface of the nanoparticles is negatively charged. The amino group of LPFFD-OH is protonated under the acidic conditions applied, thus they can be bound to the negatively charged gold surface [30]. Alternatively, the aromatic ring of phenylalanine might interact with the surface. The UV–vis spectra of LPFFD-OH modified gold

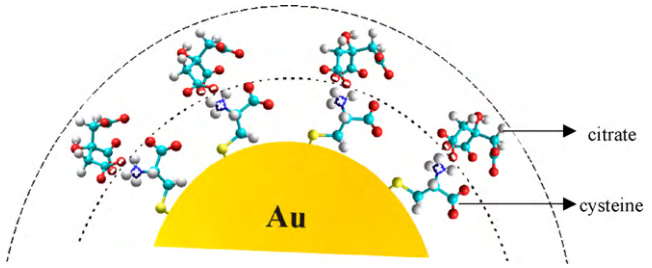

Fig. 4. Schematic representation of the formation of organic double layer structure after addition of cysteine to citrate-stabilized gold dispersion.

nanoparticles were registered and similar experimental findings were observed as in the case of the Au–cysteine system (Fig. 5a). The wavelength difference between the two plasmon maximum is quite similar for LPFFD-OH ($\Delta\lambda$ = 193 nm) than in case of the Cys-containing system ($\Delta\lambda$ = 185 nm, Fig. 1b), thus considerable structural difference could not be observed. In order to investigate the effect of the LPFFD-OH in gold dispersion containing cysteine, mixed ligand–Au systems were also studied. When LPFFD-OH was added to a cysteine-containing nanodispersion, the difference between the two plasmon maximum was ~213 nm (Fig. 5b). Although the second band at 743 nm became narrower and more intensive, the spectral parameters suggest that the presence of LPFFD-OH did not reduce the formation of aggregates considerably.

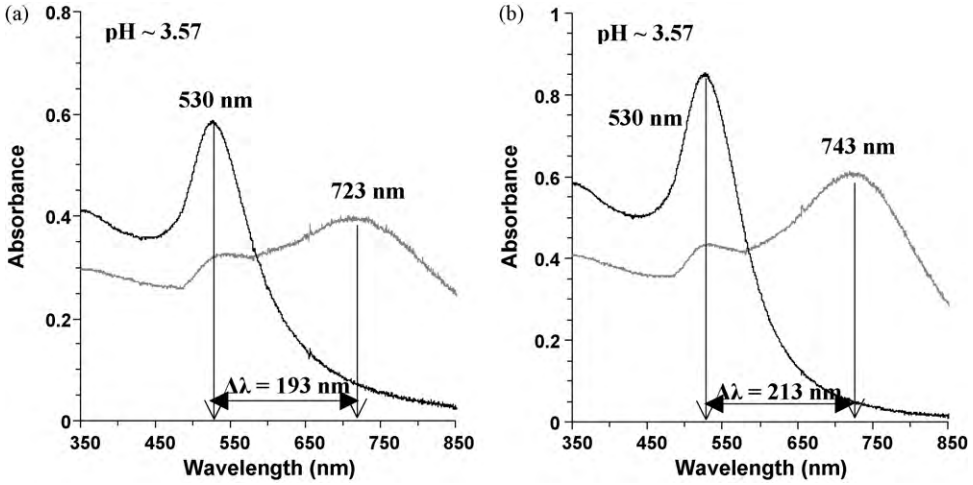

Fig. 5. UV–vis spectra of Au–LPFFD-OH (a) and Au–LPFFD-OH–cysteine systems (b) at pH ~ 3.57 (a: c_{Au} = 0.135 mM, $c_{LPFFD-OH}$ = 0.134 mM, b: c_{Au} = 0.135 mM, $c_{LPFFD-OH}$ = 0.134 mM, c_{Cys} = 0.636 mM).

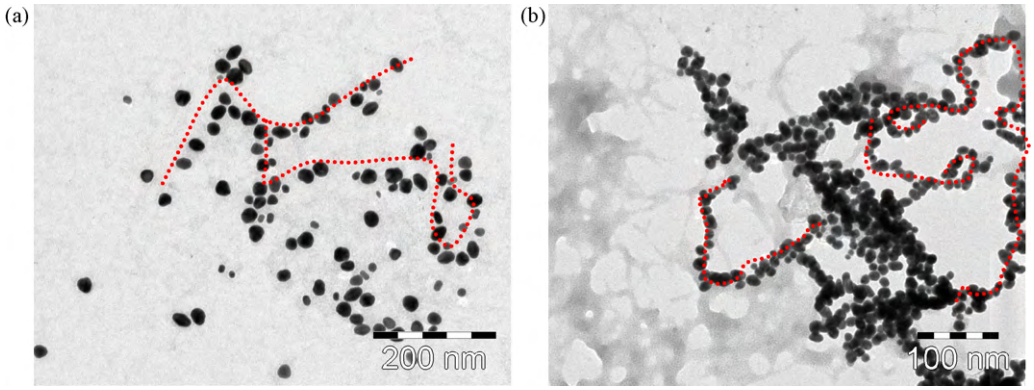

Fig. 6. TEM pictures of Au–LPFFD-OH (a) and Au–LPFFD-OH–cysteine systems (b) at different enlargements (a: c_{Au} = 0.135 mM, $c_{LPFFD-OH}$ = 0.134 mM, b: c_{Au} = 0.135 mM, $c_{LPFFD-OH}$ = 0.134 mM c_{Cys} = 0.636 mM).

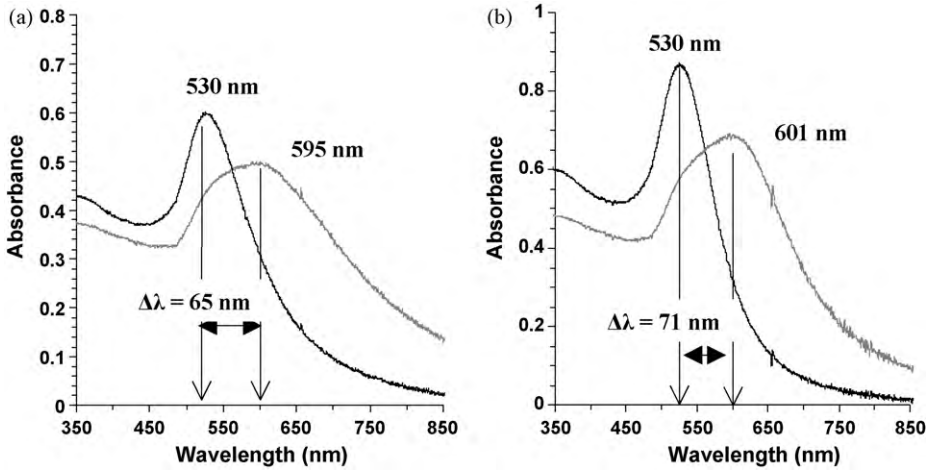

Fig. 7. UV–vis spectra of Au–Cys^{0}A$\beta_{1\text{-}28}$ (a) and Au–Cys^{0}A$\beta_{1\text{-}28}$–LPFFD-OH systems (b) (a: c_{Au} = 0.127 mM, $c_{CysA\beta(1\text{-}28)}$ = 0.0135 mM, b: c_{Au} = 0.127 mM, $c_{LPFFD\text{-}OH}$ = 0.022 mM, $c_{CysA\beta\ (1\text{-}28)}$ = 0.0135 mM).

TEM images of the above mentioned systems are shown in Fig. 6. The gold nanoparticles are arranged by the LPFFD-OH molecules (Fig. 6a), and they are placed separately from each other at 4.4 ± 2.9 nm, indicating a loose, randomly organized state. On the other hand, chain-like structures can also be observed for both systems (marked by red dashed lines in Fig. 6a and b).

Comparison of TEM images represented by Fig. 6a and b, it is also well demonstrated that the aggregation of the particles results in a coherent structure in the mixed system, but in the system containing only LPFFD-OH, direct linking points between the particles were not observed.

Beside the cysteine and LPFFD-OH, interaction of gold nanoparticles with large biomolecules like β-amyloid peptides was also investigated. A$\beta_{1\text{-}28}$ and A$\beta_{1\text{-}40}$ cannot form covalent bonds with gold. On the other hand, if they are modified by cysteine, they can bind to Au surface via thiol function. Fig. 7a represents the spectra of the Au sol (black line) and the Au–Cys^{0}A$\beta_{1\text{-}28}$ system (grey line) at ~9.5:1 noble NPs to peptide ratio. Comparison of the spectra of the cysteine- (Fig. 1b) or LPFFD-OH-containing gold dispersion (Fig. 5a), significant differences were observed in the spectra. The second plasmon maximum appeared at λ_{max} ~ 595 nm, while the band corresponding to the citrate-stabilized gold dispersion was shifted from ~530 nm to ~550 nm and these bands were overlapped with each other in the spectrum. As it can be seen in Fig. 7a, Δλ is 65 nm. When LPFFD-OH was added to the Au–Cys^{0}A$\beta_{1\text{-}28}$ system, the observed spectrum (Fig. 7b assigned with grey line) showed a similar trend to that of the Au–Cys^{0}A$\beta_{1\text{-}28}$ system. Namely, Δλ is 71 nm, but the band is somewhat narrower. These results clearly suggest that in these systems the formation of chain-like aggregates is not dominant. Instead of the chain-like arrangement of the gold nanoparticles, the presence of the larger aggregates is favoured. This theory was confirmed by TEM images. Images represented in Fig. 8a and b. clearly demonstrate a dominant association in these systems. A$\beta_{1\text{-}28}$ is substantially longer peptide than LPFFD-OH, and due to the polyelectrolyte–polyelectrolyte interaction between the side-chains of the amino acids, intermolecular association of the peptide chains is favoured resulting in an enhanced aggregation of the nanoparticles.

Interaction of gold nanoparticles with cysteine modified amyloid-β 1-40 molecules (Cys^{0}A$\beta_{1\text{-}40}$) was also studied. As it can be seen in Fig. 9a, the presence of the second band could not be observed, however the absorption band of the Au NPs (assigned with black) was shifted from ~ 520 to 538 nm in the spectrum (grey line) registered 30 min later after the addition of the peptide to gold dispersion. These results strongly suggest that formation of the aggregates was not dominant and presumably Cys^{0}A$\beta_{1\text{-}40}$ could stabilize the NPs by binding to gold surface via thiol moiety.

Comparison of the shifts between the bands observed in the spectra one can conclude, that parallel with the increase in size of the biomolecules (from cysteine to Cys^{0}A$\beta_{1\text{-}40}$), the wavelength distance is gradually decreases and the formation of aggregates is hindered. The shift was about 185 nm in case of cysteine, while β-

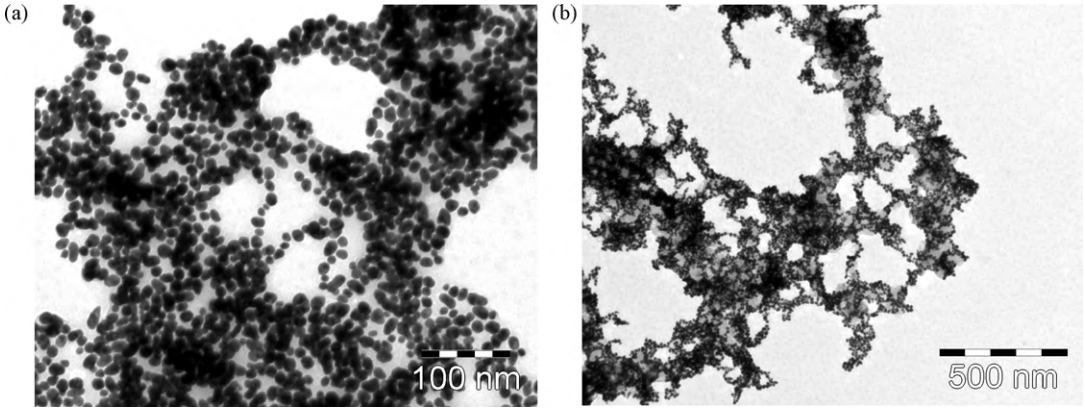

Fig. 8. TEM images of Au–Cys^{0}A$\beta_{1\text{-}28}$ (a) and Au–Cys^{0}A$\beta_{1\text{-}28}$–LPFFD-OH systems at different enlargements (b) (a: c_{Au} = 0.127 mM, $c_{CysA\beta(1\text{-}28)}$ = 0.0135 mM, b: c_{Au} = 0.127 mM, $c_{CysA\beta(1\text{-}28)}$ = 0.0135 mM, $c_{LPFFD\text{-}OH}$ = 0.022 mM).

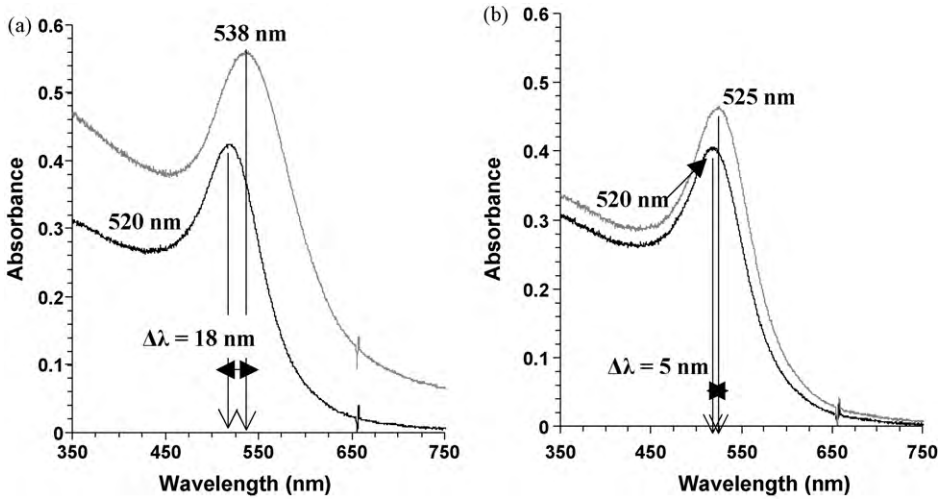

Fig. 9. UV–vis spectra of Au–Cys^{0}A$\beta_{1\text{-}40}$ (a) and Au–A$\beta_{1\text{-}42}$ systems (b) (a: c_{Au} = 0.13 mM, $c_{CysA\beta(1\text{-}40)}$ = 0.0127 mM, b: c_{Au} = 0.13 mM, $c_{A\beta\,(1\text{-}42)}$ = 0.0035 mM).

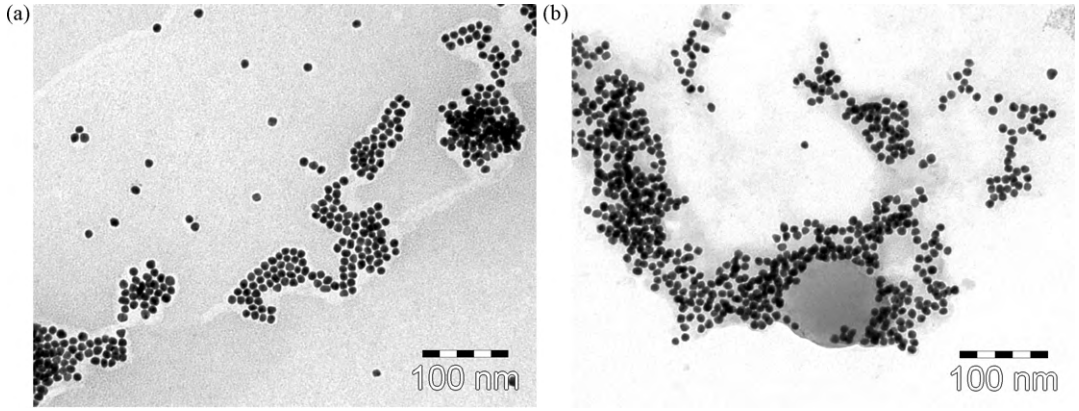

Fig. 10. TEM pictures of citrate-stabilized gold dispersion (a) and Au–A$\beta_{1\text{-}42}$ systems (b) (a: c_{Au} = 0.13 mM, b: c_{Au} = 0.13 mM, $c_{A\beta\,(1\text{-}42)}$ = 0.0035 mM).

amyloid, which contains more than 40 amino acids, caused only a ~18 nm plasmonic shift.

The direct interaction between A$\beta_{1\text{-}42}$ (peptide without cysteine) and gold particles was also measured and the observed shift was only ~5 nm (Fig. 9b). As it can be seen, the second band corresponding to the presence of aggregates does not exist. This effect might be due to the size of molecules, namely large biomolecules can compass gold NPs around whereby the aggregation would be inhibited. A$\beta_{1\text{-}42}$ molecules without cysteine can bind to the surface of gold nanoparticles via both the apolar and the N-donors containing side-chains. TEM images of gold NPs in the absence (Fig. 10a) and the presence of amyloid 1-42 (Fig. 10b) can be seen in Fig. 10. Significant difference between the images of dispersions containing monodisperse gold NPs either with or without Au–A$\beta_{1\text{-}42}$ could not be observed. By the comparison of the TEM images (Figs. 2b, 6, 8 and 10b), it can be concluded, that formation of aggregates could be detected in most cases, except in the Au–A$\beta_{1\text{-}42}$ system. These results suggest that stable Au–A$\beta_{1\text{-}42}$ bioconjugates are formed at the applied concentrations (Au:A$\beta_{1\text{-}42}$ ~ 37:1 molar ratio).

4. Conclusions

Interaction of cysteine, LPFFD-OH and β-amyloid peptides like Cys^{0}A$\beta_{1\text{-}28}$, Cys^{0}A$\beta_{1\text{-}40}$ and A$\beta_{1\text{-}42}$ with gold nanoparticles (d_{Au} = 13.6 ± 4.7 nm average diameter) have been studied by UV–vis spectrophotometry, DLS measurements and TEM investigations. In the case of cysteine functionalization, ^{1}H NMR spectra were also recorded to characterize the position of the citrate and cysteine on the gold surface. Results strongly suggest that in the cysteine- and LPFFD-OH containing gold dispersions, formation of aggregates with chain-like structure is probable. Due to the addition of cysteine to citrate-stabilized gold aqueous dispersion, the citrate molecules are replaced by cysteine resulting in the formation of a organic double layer structure.

Parallel with the increase of the size of the biomolecules (from cysteine to β-amyloid peptides), the degree of aggregation is gradually decreases. In the case of Au–A$\beta_{1\text{-}42}$ systems, the aggregation process is completely eliminated.

Acknowledgements

The authors are very thankful for the financial support of the Hungarian Scientific Research Fund OTKA Nr. K 73307, OTKA Nr. NK 73672 and Memoload (FP-7 201 159).

L. Fülöp wishes to thank the Hungarian Academy of Sciences for the support of the János Bolyai Research Grant.

References

[1] J. Turkevich, Gold Bull. 3 (1985) 18.
[2] Y. Shao, Y. Jin, S. Dong, Chem. Commun. 9 (2004) 1104.
[3] T. Jensen, L. Kelly, A. Lazarides, G.C. Schatz, J. Cluster Sci. 10 (2) (1999) 295.
[4] V. Sharma, K. Park, M. Srinivasarao, Mater. Sci. Eng. R 65 (2009) 1.
[5] R.M. Bright, D.G. Walter, M.D. Musick, et al., Langmuir 12 (1996) 810.

[6] R. Elghanian, J.J. Storhoff, R.C. Mucic, R.L. Letsinger, C.A. Mirkin, Science 277 (1997) 1078.
[7] R. Elghanian, J.J. Storhoff, R.C. Mucic, R.L. Letsinger, C.A. Mirkin, Langmuir 12 (1996) 810.
[8] R.C. Triulzi, Q. Dai, J. Zou, R.M. Leblanc, Q. Gu, J. Orbulescu, Q. Hou, Colloids Surf. B: Biointerfaces 63 (2008) 200.
[9] Z. Zhong, S. Patskovsky, P. Bouvrette, H.T. Luong, A. Gedanken, J. Phys. Chem. B 108 (2004) 4046.
[10] S. Aryal, K.C. Remant Bahadur, N. Dharmaraj, N. Bhattarai, C.H. Kim, H.Y. Kim, Spectrochim. Acta A 63 (2006) 160.
[11] S. Aryal, K.C. Remant Bahadur, N. Bhattarai, C.K. Kim, H.Y. Kim, J. Colloid Interface Sci. 299 (2006) 191.
[12] F. Porta, G. Speranza, Z. Krpetic, V.D. Santo, P. Francescato, G. Scari, Mater. Sci. Eng. B 140 (2007) 187.
[13] C.W. Cairo, A. Strzelec, R.M. Murphy, L.L. Kiessling, Biochemistry 41 (2002) 8620.
[14] M.J. Kogan, N.G. Bastus, R. Amigo, D.G. Bosch, et al., Nano Lett. 6 (1) (2006) 110.
[15] I. Olmedo, E. Araya, F. Sanz, E. Medina, J. Arbiol, et al., Bioconjug. Chem. 19 (2008) 1154.
[16] S. Boussert, I. Diez-Perez, M.J. Kogan, E. de Oliveira, E. Giralt, ACS Nano 3 (10) (2009) 3091.
[17] M. Pérez, R. Cuadros, M.J. Benitez, J.S. Jiménez, J. Alzheimer Dis. 6 (2004) 461.
[18] K. Hasegawa, K. Ono, M. Yamada, H. Naiki, Biochemistry 41 (2002) 13489.
[19] W.P. Hu, G.L. Chang, S.J. Chen, Y.M. Kuo, J. Neurosci. Methods 154 (2006) 190.
[20] M.S. Liu, H.M. Chiu, F.J. Fan, H.T. Tsai, S.S. Wang, Y. Chang, W.Y. Chen, Colloids Surf. B Biointerfaces 58 (2007) 231.
[21] J. Ryu, H.-A. Joung, M.-G. Kim, C.B. Park, Anal. Chem. 80 (2008) 2400.
[22] T. Ariga, K. Kobayashi, A. Hasegawa, M. Kiso, H. Ishida, T. Miyatake, Arch. Biochem. Biophys. 388 (2001) 225.
[23] M. Hirohata, K. Hasegawa, S. Tsutsumi-Yasuhara, Y. Ohhashi, T. Ookoshi, K. Ono, M. Yamada, H. Naiki, Biochemistry 46 (2007) 1888.
[24] Y. Yan, Y. Liu, M. Sorci, G. Belfort, J.W. Lustbader, S.S. Yan, C. Wang, Biochemistry 46 (2007) 1724.
[25] M.J. Pérez de Vega, J.L. Baeza, M.T. Garcia-López, M. Vila-Perelló, C. Jiménez-Castells, A.M. Simón, D. Frechilla, J. del Río, R. Gutiérrez-Gallego, D. Andreu, R. González-Muniz, Bioorg. Med. Chem. Lett. 18 (2008) 2078.
[26] M.I. Aguilar, D.H. Small, Neurotox. Res. 7 (2005) 17.
[27] Z. Chen, G. Krause, B. Reif, J. Mol. Biol. 354 (2005) 760.
[28] M. Zarándi, K. Soós, L. Fülöp, Zs. Bozsó, Zs. Datki, G.K. Tóth, B. Penke, J. Peptide Sci. 13 (2007) 94.
[29] S.H. Brewer, W.R. Glomm, M.C. Johnson, M.K. Knag, S. Franzen, Langmuir 21 (2005) 9303.
[30] M. Geneviéve, C. Vieu, R. Carles, A. Zwick, G. Briére, L. Salomé, E. Trévisiol, Microelectron. Eng. 84 (2007) 1710.